

# A Molecular Dynamics Study of the Structural Stability of HIV-1 Protease Under Physiological Conditions: The Role of Na<sup>+</sup> Ions in Stabilizing the Active Site

Dmytro Kovalskyy,<sup>1\*</sup> Volodymyr Dubyna,<sup>1</sup> Alan E. Mark,<sup>2</sup> and Alexander Kornelyuk<sup>1</sup>

<sup>1</sup>Protein Engineering Department, Institute of Molecular Biology and Genetics, UAS, Kiev, Ukraine

<sup>2</sup>Laboratory of Biophysical Chemistry, University of Groningen, Groningen, The Netherlands

**ABSTRACT** HIV-1 protease is most active under weakly acidic conditions (pH 3.5–6.5), when the catalytic Asp25 and Asp25' residues share 1 proton. At neutral pH, this proton is lost and the stability of the structure is reduced. Here we present an investigation of the effect of pH on the dynamics of HIV-1 protease using MD simulation techniques. MD simulations of the solvated HIV-1 protease with the Asp25/25' residues monoprotinated and deprotonated have been performed. In addition we investigated the effect of the inclusion of Na<sup>+</sup> and Cl<sup>-</sup> ions to mimic physiological salt conditions. The simulations of the monoprotinated form and deprotonated form including Na<sup>+</sup> show very similar behavior. In both cases the protein remained stable in the compact, “self-blocked” conformation in which the active site is blocked by the tips of the flaps. In the deprotonated system a Na<sup>+</sup> ion binds tightly to the catalytic dyad shielding the repulsion between the COO<sup>-</sup> groups. *Ab initio* calculations also suggest the geometry of the active site with the Na<sup>+</sup> bound closely resembles that of the monoprotinated case. In the simulations of the deprotonated form (without Na<sup>+</sup> ions), a water molecule bound between the Asp25 Asp25' side-chains. This disrupted the dimerization interface and eventually led to a fully open conformation. *Proteins* 2005;58:450–458.

© 2004 Wiley-Liss, Inc.

**Key words:** HIV-1 protease; molecular dynamics; acidic and neutral pH; positive ions; stabilizing factor; *ab initio* optimization

## INTRODUCTION

HIV-1 protease is a homodimer formed by 2 chains of 99 amino acid residues each. HIV-1 PR belongs to the class of aspartic retrovirus proteinases that are characterized by a highly conserved catalytic triad Asp25(25')-Thr26(26')-Gly(27'). The loss of either the Asp25 or Asp25' residues in the dimer results in the complete loss of enzymatic activity. Both monomers contribute equally to the dimer, which in the unbound state exhibits C2-symmetry. Both subunits provide catalytic amino acids, which are located at the base of the active site (see reviews<sup>1,2</sup>). Two β-hairpins, the so-called flaps, cover and control the access to the active site. In the crystal structure of the unbound form of HIV-1 PR, the dimer has a horseshoe-like shape (semiopen

conformation) with strong intersubunit interactions toward the bottom of the structure and weak interactions between the flaps at the top of the enzyme (see Fig. 1).<sup>1–4</sup> When a substrate binds to the active site, the flaps close over a ligand (closed conformation) and the structure of the protease becomes more torus-like. Note that the semiopen conformation corresponds neither to the substrate bound complex nor would permit the ligand to enter into active site. It has been suggested, therefore, that semiopen conformation results from crystal packing effects.<sup>5</sup>

HIV-1 PR is of great pharmaceutical importance, because it is required for the formation of mature virions<sup>6</sup> and, as such, has been the focus of numerous experimental and theoretical studies. In particular, the mechanism of action and nature of the active site has attracted much debate. Initially, a nucleophilic mechanism for the aspartic proteinases was proposed.<sup>7</sup> This mechanism implies formation of the covalently bonded HIV-1 PR-substrate complex during the course of reaction. There is as yet no direct experimental support for this mechanism, although recent, state-of-the-art computational studies do indicate that a direct nucleophilic reaction is feasible.<sup>8,9</sup> In contrast, the GA/GB mechanism as originally proposed by Fruton<sup>10</sup> appears supported by numerous studies.<sup>11–22</sup> According to the GA/GB mechanism, a lytic water molecule takes part in the reaction. Common to both these mechanisms is the requirement that one of the catalytic Asps be charged while the other neutral. In line with this, the stability and reactivity of HIV-1 PR as a function of pH is bell-shaped between pH ~3.5 and ~6.5 (weak acidic

*Abbreviations:* AMD, Advanced Micro Devices; GA/GB, general acid–general base; HIV-1 PR, Retroviral protease from the human immunodeficiency virus type 1; MD, molecular dynamics; PDB, Protein Data Bank; PME, particle mesh Ewald; RHF, Restricted Hartree-Fock; RMSD, root-mean-square deviation; SPC, simple point charge.

The Supplementary Materials referred to in this article can be found at <http://www.interscience.wiley.com/jpages/0887-3585/suppmat/index.html>

Grant sponsor: The European Science Foundation (<http://www.esf.org/>) program “Challenges in Molecular Simulations: Bridging the time-scale and length-scale gap” (SIMU).

\*Correspondence to: Dmytro Kovalskyy, Institute of Molecular Biology and Genetics, 150 Akad. Zabolotnogo Street, Kiev-143, 03143 Ukraine. E-mail: dikov@imbg.org.ua

Received 12 December 2003; Accepted 30 June 2004

Published online 23 November 2004 in Wiley InterScience ([www.interscience.wiley.com](http://www.interscience.wiley.com)). DOI: 10.1002/prot.20304

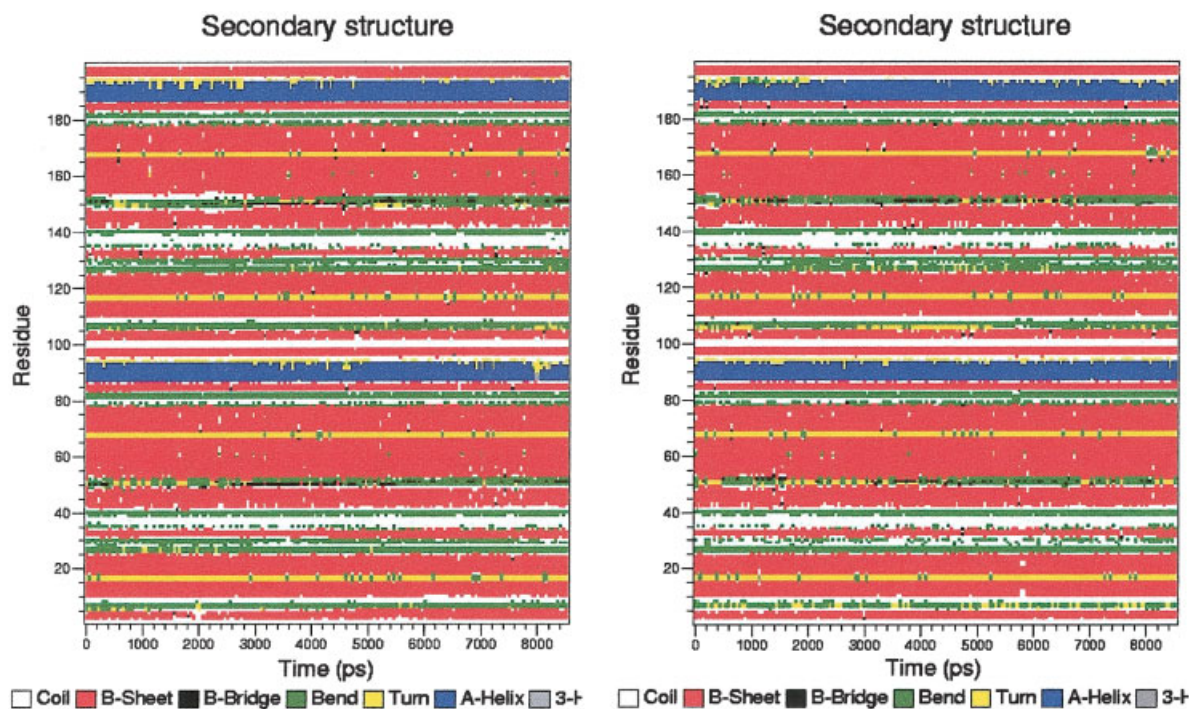


Fig. 1. A schematic representation of the secondary structure of HIV-1 protease from the systems Asp (left) and AspH (right) as a function of time.

pH), with the maximum stability and enzymatic activity occurring at pH  $\sim 5-6$ .<sup>11,23-25</sup> It is believed that the 2 residues share a proton under weakly acidic conditions and are chemically equivalent in the unbound state. The most widely accepted model based on the GA/GB mechanism is one in which a proton is attached to the outer oxygen of the Asp25' (close to scissile peptide carbonyl group) and a lytic water molecule forms bifurcated hydrogen bonds with inner oxygen atoms of the Asp25/25',<sup>11,15,22,24,26-33</sup> although other arrangements have been proposed.<sup>9,34</sup>

Besides the role of the protonation state of Asp25 or Asp25' in catalysis, pH is a major determining factor in the stability of the protein and the binding of inhibitors.<sup>35-38</sup> Depending on the particular inhibitor, various configurations of the HIV-1 protease active site could be suggested.<sup>26,28-31,33,38</sup> In particular, the suggestion is that specific inhibitors bind to different protonation states of the catalytic dyad. Certainly, the binding of some inhibitors increases the structural stability of the protease<sup>39,40</sup> and can be associated with a shift in the pKa of the Asp25/25' dyad.<sup>31</sup> Kinetic and thermodynamic studies of the unbound protease show that the protease is most stable at weakly acidic pH, where the Asp dyad is monoprotated.<sup>4,11,23-25,41,42</sup> There is, however, little direct experimental data on what structural changes (if any) accompany deprotonation. The conformational flexibility of the active-site unbound HIV-1 protease has been addressed in a number of fluorescent, computational, and NMR studies.<sup>43-57</sup> In particular the stability of the dimer<sup>52</sup> and the opening of the flap<sup>47</sup> have been examined as a function of pH. A consistent picture, however, has yet to

emerge. For example, based on NMR experiments<sup>55,56</sup> it was suggested that, in solution, HIV-1 protease could best be described as ensemble of predominantly semiopen conformations, but the existence of closed conformations could not be excluded. In contrast, in the MD simulations of Scott and Schiffer,<sup>54</sup> only a fully open conformation was obtained. The flaps opened after just 3 ns of the simulation and remained stable for an additional 7 ns (total 10 ns). The NMR data were, however, obtained at slightly acidic pH (the Asp dyad is monoprotated), whereas in the MD study, the Asp25 and the Asp25' residues were deprotonated.

It is clear from the above that there remains much uncertainty in regard to the effect that the protonation state of the catalytic dyad has on the structural stability and conformational flexibility of the protease. For this reason, we have performed a systematic investigation of the influence of the Asp25/Asp25' protonation state on the dynamics of the protease at an atomic level. Our aim was to understand in detail the factors that may stabilize or destabilize the protease at neutral pH as compared with weakly acidic pH. In contrast to previous studies, we have attempted to work close to physiological conditions. To this end, we have performed a series of MD simulations of the unbound HIV-1 PR, in which the catalytic residues are monoprotated and deprotonated catalytic residues in the presence of  $\text{Na}^+$  and  $\text{Cl}^-$  ions to mimic a 0.15 M salt concentration.

## MATERIALS AND METHODS

### Molecular Dynamics Simulations

All simulations and trajectory analysis were performed with a parallel implementation<sup>58</sup> of the GROMACS<sup>59</sup>

package in conjunction with the GROMOS96 force field.<sup>60</sup> The Verlet integration scheme (leapfrog)<sup>61</sup> was used, together with a 2-fs timestep. The PME<sup>62</sup> algorithm was applied to treat long-range electrostatics, and a twin-range cutoff was used for the van der Waals interactions. Interactions within 0.9 nm were updated every step, while those within 1.4 nm were updated only every 10 steps, together with the pair list. All bonds within the protein bonds were constrained using the SHAKE<sup>63</sup> algorithm. The SETTLE<sup>64</sup> procedure was to constrain the SPC water molecules. The temperature and the pressure were maintained by coupling temperature and pressure baths using the method of Berendsen et al.,<sup>65</sup> with relaxation times of 0.1 ps and 0.5 ps, respectively. The pressure was adjusted to 1 atm with compressibility of  $4.5 \times 10^{-5} \text{ bar}^{-1}$ . All the simulations were performed at 310 K (body temperature).

Three MD simulations were performed: (1) HIV-1 PR with monoprotonated Asp25/25' residues (AspH system) at a physiological salt concentration; (2) HIV-1 PR with the deprotonated residues (Asp system) at a physiological salt concentration; and (3) the protease with the deprotonated catalytic dyad, but with only 5 Cl<sup>-</sup> counterions included (Asp\_cions system). For the AspH system, the active site was constructed in accordance with previous ab initio calculations.<sup>33</sup> The proton was arbitrarily attached to the Oδ1 oxygen of the Asp25 (note that, in principle, there is no difference between the Asp25 and Asp25' residues in the dimer) and the water "Wat\_b" was oriented to form equivalent hydrogen bonds with both Oδ2 atoms of the Asp25 and Asp25' residues. For each of the systems, the following procedure was applied unless stated otherwise. The 1hhp structure<sup>66</sup> from the PDB<sup>67</sup> was used as initial configuration. The system was subjected to 200 steps of steepest descent energy minimization. The protease was placed in an octahedron box. The minimal distance between protein and the box wall was 1 nm. The box was then filled with SPC water molecules (11,571 water molecules).<sup>68</sup> A 50-ps simulation, in which all protein atoms were positionally restrained, was performed to relax the solvent. The GENION procedure from GROMACS package was then used to replace water molecules that have most favorable electrostatic potential by ions Na<sup>+</sup> and Cl<sup>-</sup>. In order to mimic physiological salt concentration 34 Cl<sup>-</sup> and 29 Na<sup>+</sup> ions were added to AspH system, whereas to the Asp system, 33 Cl<sup>-</sup> and 29 Na<sup>+</sup> ions were inserted. For the Asp\_cions system, only 4 Cl<sup>-</sup> ions were inserted. The resulting systems were electrically neutral overall. The systems were again energy-minimized and a further 100-ps simulation with position restraints was performed at 310 K. New velocities were then generated. The Asp and AspH systems were simulated for 8.5 ns. The Asp\_cions system was simulated for 8 ns. Data were recorded each 1 ps. All simulations were performed in parallel using a cluster of 4 dual-processor AMD-based machines.

### Ab Initio Calculations

Ab initio calculations were performed using PC GAMESS,<sup>69</sup> a PC-optimized implementation of the GAMESS program.<sup>70</sup> An initial configuration was con-

structed based on the 1hhp protein structure. Leu24(carbonyl group only)-Asp25-Thr26-Gly27 residues from each chain were treated explicitly in order to describe the active site without constraints. In the AspH system, a proton and "Wat\_b" were placed as described above for the MD simulations, in accordance with the method of Geller et al.<sup>33</sup> In the Asp system, the "Wat\_b" water was replaced by a Na<sup>+</sup> ion (at the oxygen atom position). A RHF geometry optimization procedure with 6-31+G(d,f)<sup>71-73</sup> basis set was then performed.

### Calculations of the Generalized Order Parameters

The model-free formalism of Lipari-Szabo<sup>74,75</sup> was used for the calculation of the generalized order parameter of a peptide N-H bond vector. In order to remove the rotational motion of the protein, a least-squares fit of the C<sub>α</sub>-atoms to the initial structure was performed for each frame. The calculations were performed using the expression<sup>76</sup>

$$S^2 = \sum_{k=i}^j \sum_{l=j}^i p_{eq}(k) p_{eq}(l) P_2(\cos \phi_{kl}),$$

where  $S^2$  is a generalized order parameter,  $\phi_{kl}$  is the angle between N-H bond directions in the  $k$ - and  $l$ -states,  $P_2$  is the second order Legendre polynomial, and  $p_{eq}(i)$  is the probability of the  $i$ th state.  $S^2$  is a measure of backbone flexibility (the movement of the axis is anisotropic if  $S^2 = 0$ , and the axis is rigid if  $S^2 = 1$ ). The trajectory of the Asp system was divided into 100-ps windows; the order parameter was calculated for each window separately, and the  $S^2$  value was averaged over all windows. Errors were estimated from the variance of the values between different windows.

### Graphical and Structural Analysis

The SPDBV,<sup>77</sup> Molekel,<sup>78</sup> and VMD<sup>79</sup> programs were used for trajectory visualization and graphical structure analysis. A WASP<sup>80</sup> code was used in order to check a possibility to find Na<sup>+</sup> ions in HIV-1 protease crystal structures. The DSSP<sup>81</sup> program was used to evaluate the secondary structure content.

## RESULTS AND DISCUSSION

### Global Structural Flexibility

Figure 1 shows a plot of the secondary structure as a function of time for the simulations Asp and AspH. As can be seen, well-ordered secondary structure elements (e.g.,  $\beta$ -sheets and  $\alpha$ -helix) remain stable throughout the simulation. The C $\alpha$  RMSD from the experimental X-ray structure [Fig. 2(a)] and the radius of gyration [Fig. 2(b)] also show that, at least for the period simulated (8.5 ns), the Asp and AspH systems behave in an almost identical fashion. Other factors investigated, such as the nature of the solvent accessible surface area and the hydrogen-bonding pattern (data not shown), are also similar for the two systems. Overall, the conformation of the protease remains close to that of the crystal structure. The largest deviations are observed in the tips of the flaps (Fig. 3). A

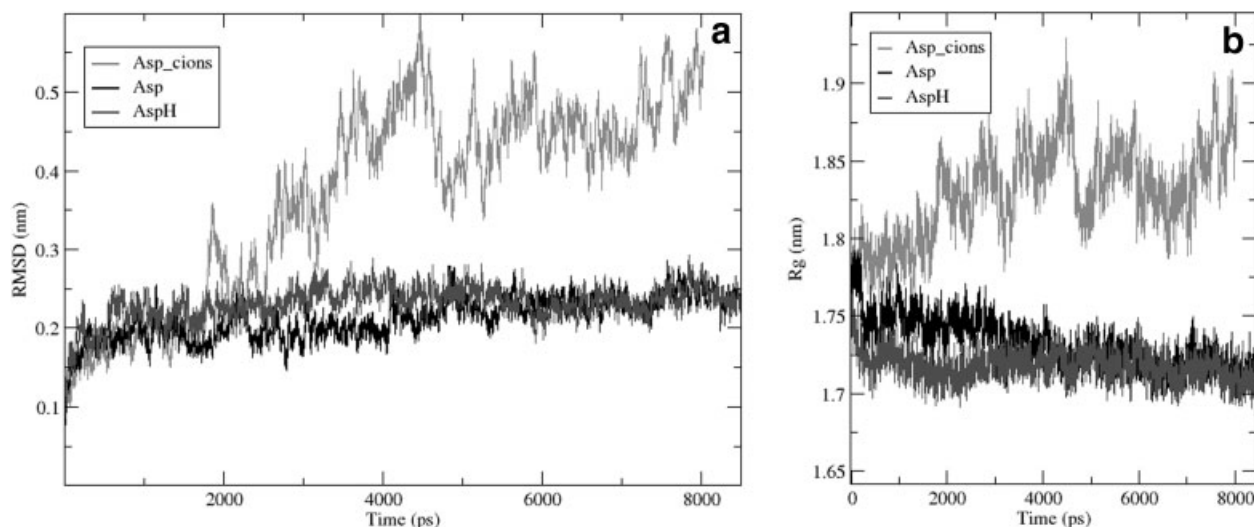


Fig. 2. RMSD (a) and gyration radius (b) of  $C\alpha$  atoms of HIV-1 protease in Asp, AspH, and cions simulations.



Fig. 3. Superposition of the final conformations from Asp (black) and AspH (dark gray) simulations on the initial crystal structure (light gray). Note the similarity between the final structures and that the flap tips curl in and, thus, block access to the active site.

slight inward shift of the top part of the protease is also evident. The RMSD of  $C\alpha$  atoms the final configurations from the Asp and AspH simulations is only 0.14 nm. This difference is significantly less than the deviation of both structures from the starting X-ray structure,  $\sim 0.25$  nm. All of the above suggest that the Asp and AspH simulations behave in an almost identical fashion.

### Flap Motion

In both the Asp and AspH trajectories, the flaps are the most flexible part of the protein. Three distinct types of motion could be distinguished: (1) concerted motion of residues 39–60 [Fig. 4(a)]; (2) rotation of flaps (residues 45–55) around an axis along the b-hairpin structure [Fig. 4(b)]; and (3) the flipping of the tips of the flap (residues 48–53) [Fig. 4(c)]. In both simulations, a compact “self-blocked” conformation forms after 4 ns that remains stable thereafter. In this conformation, the flaps approach the catalytic Asp25 and Asp25' residues and block completely

access to the active site (Fig. 3 and Fig. 1 of Supplemental Material). Additional inter- and intrasubunit interactions form with the side-chain of Ile50 interacting with the side-chains of Pro80, Val82, and Ile84 residues [Fig. 5(a)]. These residues belong to a flexible loop (residues Gly78–Ile84). Forming these interactions does not require any significant change in the conformation of the flap or of the protein as a whole. However, the formation of this cluster may also provide a hydrophobic environment for the isoleucines within the tips of the flap and thus contribute to the overall stability of the dimer. We note that the Val82Phe mutant is more than 100 times less stable than the wild-type.<sup>82</sup> Structural studies of the Val82Phe mutant complexed with cyclic urea inhibitors suggest that the phenyl ring is not directed toward the active site but instead forms external hydrophobic contacts with Leu10 and Val23, or with the inhibitor itself. As such, it would not be available to interact with Ile50, as seen in the simulations, and could explain the marked decrease in stability seen in the Val82Phe mutant. On average, only 1.55 hydrogen bonds are formed between the 2 flap tips during the simulations, and no specific hydrogen bond could be considered as stable [Fig. 5(b)]. Our results on the HIV-1 protease flexibility are in agreement with thermodynamic studies of the HIV-1 protease by Freire and coworkers,<sup>4,39</sup> who suggested that residues 33–60 (from each chain) comprise the most labile part of the protein.<sup>4</sup> However, upon ligand binding, the flaps become highly ordered and structurally stable.<sup>39</sup> The flexibility of the flaps of HIV-1 protease has also been studied by Freedberg et al. using NMR techniques.<sup>56</sup> They concluded that on a nanosecond timescale, substantial motion in the flaps is restricted to residues 27–41 and 49–53 at the tips of the flaps, and suggested that the fast fluctuations reflect a dynamic equilibrium between semiopen and possibly closed conformations. The “self-blocked” conformation can be seen as an intermediate between these 2 conformations, if the tips of the flaps are excluded. As a way of comparing the results of

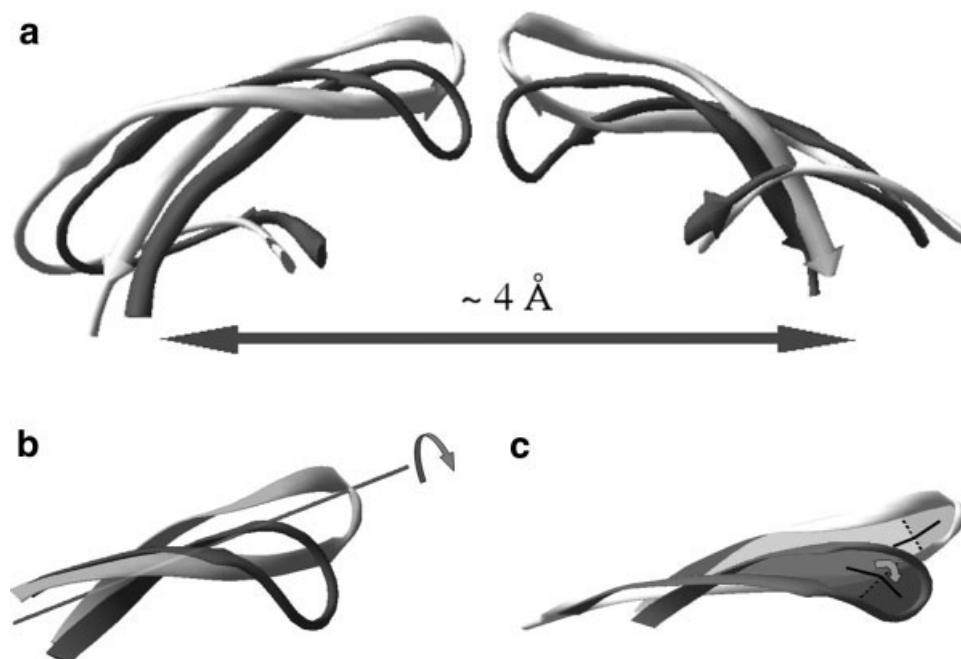


Fig. 4. Contributions to the flap motions. The initial backbone positions are colored in light gray, the final positions in dark gray. The directions of the motion are indicated by the arrows. (a) Global motions of residues 39–60 from both subunits. (b) Rotation of residues 45–55 around an axis along the  $\beta$ -hairpin structure. The residues rotate up to  $\sim 110^\circ$  of the space, while residues outside the 45–55 region are not sensitive to the motion. (c) Flipping of residues 48–53. These residues form a plane that moves relative to the plane of the other flap residues. These planes are shaded in the corresponding flap colors.

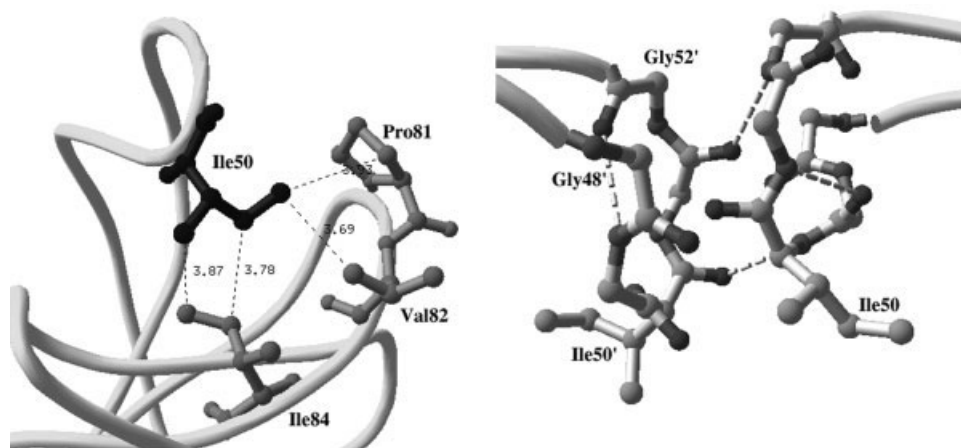


Fig. 5. Interactions within the tips of the flaps. (a) Intrasubunit, hydrophobic interaction of Ile50 with Pro81, Val82, and Ile84 residues.  $C\delta$  atom of Ile50 points toward the ring of Pro81 but also interacts with Val82. The Ile50 interacts tightly with Ile84. (b) Intersubunit hydrogen bond and van der Waals interactions of the backbone atoms of Gly48 and Gly52 within the tips of the flap. The amide groups orient in order to form favorable hydrogen bond and van der Waals interactions. On average, 1.55 hydrogen bonds are formed.

the simulations with the available NMR data,<sup>56</sup> the  $S^2$ -generalized order parameters for the protease from the Asp system have been calculated and are plotted in Figure 6, together with the experimental results. As can be seen, there is general agreement between the values predicted in the simulations and those obtained experimentally (correlation coefficient 0.6), suggesting the simulations are a reasonable representation of the degree of motion found in solution.

### The Active Site

In the simulations, almost identical results were obtained for the Asp and AspH systems. This is in contrast to previous MD simulation studies<sup>54</sup> and what might be initially expected based on some NMR studies.<sup>55,56</sup> Considering the active site of the Asp and AspH systems in more detail, we see that in the AspH system, the initial coplanar configuration of the Asp25 and Asp25' carboxylic groups

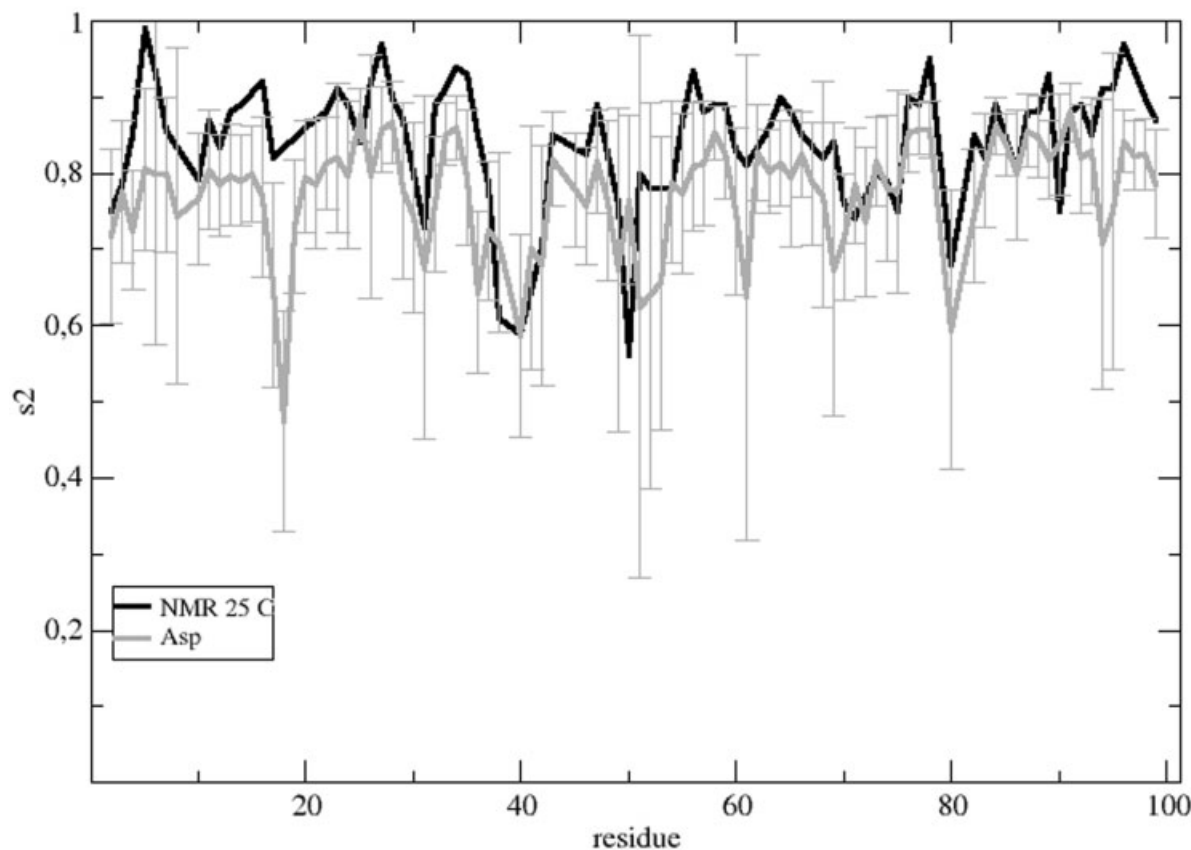


Fig. 6. Comparison of NMR order parameter  $S^2$  from the experiment (black line) and from the MD simulation of the Asp system (light gray line). The estimated error for calculated  $S^2$  from the Asp system is shown as bars.

(see Material and Methods section) is not preserved. Instead, the Asp25 and Asp25' carboxylic groups rotate around C $\beta$ -C $\gamma$  bond, and the environment of the proton becomes more tetrahedral with interactions to the 4 carboxylic oxygen atoms of Asp25 and Asp25'. A similar tendency for the carboxylic groups to rotate was observed in previous MD simulations of the HIV-1/substrate complex, where the proton was detached from the Asp25/25' residues.<sup>83</sup> However, this change could be related to limitations of the classical force field when describing charge-dipole interactions.

In the simulations of the Asp system, we found that a Na<sup>+</sup> ion bound between the Asp25 and Asp25' carboxylic groups (see Fig. 7). The position of the Na<sup>+</sup> ion is similar to that of the H<sup>+</sup> in the work of Harrison and Weber<sup>83</sup> or the oxygen of "Wat\_b" in the studies of Piana and Carloni.<sup>32</sup> The average distance between the carboxylic oxygens and the Na<sup>+</sup> ion was  $\sim 0.25$  nm. Once bound, the Na<sup>+</sup> ion did not exchange either with a water molecule or another Na<sup>+</sup> ion during the simulation. As an independent check of whether it was possible for a sodium ion to have bound instead of the "Wat\_b" water molecule in crystal structures of the free protease, the WASP program<sup>36</sup> was used to scan the HIV PR database.<sup>84</sup> The result was negative. We note, however, that as all the crystals were obtained under weak acidic pH, where Asp dyad is monoprotonated, a negative result was not surprising.

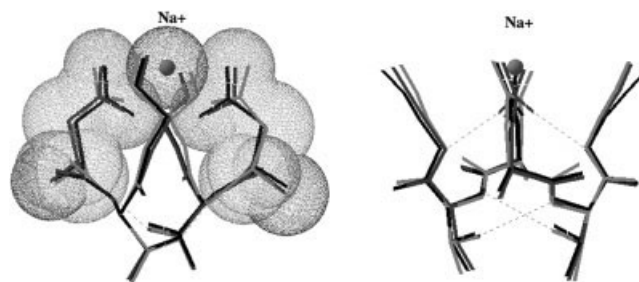


Fig. 7. Superposition of the active-site configuration from ab initio calculations (Asp system shown in black, AspH in dark gray) onto the crystal structure (light gray). For clarity, only heavy atoms are shown. The Na<sup>+</sup> ion from the Asp system is drawn as a ball. The similarity of the AspH and Asp systems is evident.

As another indication of the relative stability of the different states, ab initio geometry optimizations were performed for the AspH and Asp active sites. A superposition of the optimized active sites from the final configurations of the Asp and AspH systems onto crystal structure are shown in Figure 7. The close similarity of the active-site geometry from Asp and AspH systems suggests that Na<sup>+</sup> could substitute for H<sup>+</sup> and "Wat\_b"<sup>33</sup> at the neutral pH. Studies<sup>11,23-25</sup> indicate that the structural stability of the protease is highest when only one of the active-site residues Asp25 or Asp25' is protonated. In the simulations of the Asp system, we find that once 1 Na<sup>+</sup> ion has bound,

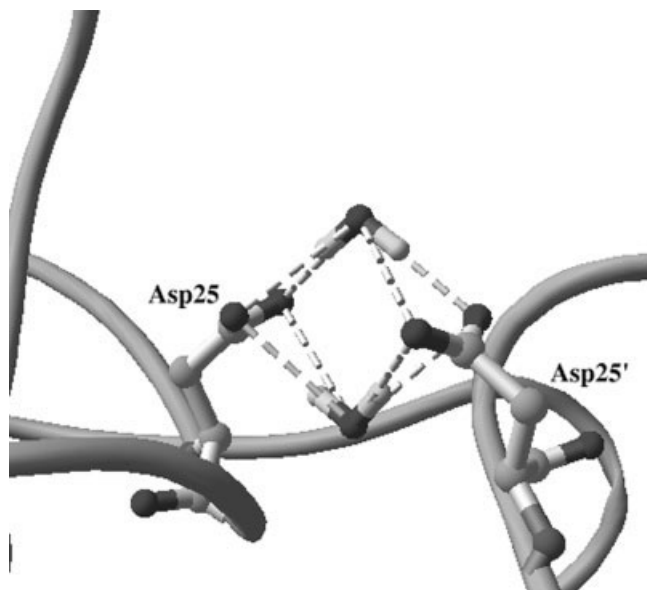


Fig. 8. Structure of the active site in the Asp\_cions simulation (5 ps). One water molecule binds up and the other binds down between the Asp25 and Asp25' side-chains. Each carboxylate oxygen atom forms hydrogen bonds with both waters.

no other  $\text{Na}^+$  ions were observed in close proximity to the catalytic dyad.

Experimentally,  $\text{Na}^+$  does not inhibit HIV-1 protease.<sup>85</sup> This does not, however, exclude the possibility that the  $\text{Na}^+$  ion could also bind at the active site. The GA/GB catalytic mechanism requires a proton and a lytic water molecule for enzymatic activity. At neutral pH, Asp25 and Asp25' are deprotonated; the proton must bind to the catalytic dyad upon or after a ligand binding to the active site. So long as the affinity for the  $\text{Na}^+$  ion is significantly lower than the affinity for the proton, the  $\text{Na}^+$  ion will be replaced with hydrogen ion upon ligand binding. In contrast, earlier experimental and theoretical works have shown that  $\text{Zn}^{2+}$  can bind to the active site and does competitively inhibit enzymatic activity at neutral pH.<sup>85–87</sup> As a divalent transition metal cation,  $\text{Zn}^{2+}$  is expected to interact much more strongly with the Asp oxygens than  $\text{Na}^+$ .

### Conformational Flexibility of Asp\_cions System

To examine the possible importance of other interactions between Asp25/25' residues and the environment, one simulation of the HIV-1 protease with only 4  $\text{Cl}^-$  counterions (Asp\_cions) was performed. In this case, a water molecule rapidly bound between, but below, the side-chains of the Asp25/25' residues (Fig. 8). The carboxylic groups turned such that each of the 4 oxygen atoms formed an equal hydrogen bond with the bound water molecule. A second water molecule also bound in a similar fashion above the carboxylic groups, forming a symmetric complex. In contrast to the first water molecule, it did not exchange with other water molecules; during the first 4.4 ns, the second water molecule was quite labile. In addition, after  $\sim 1.7$  ns, the structure began to deviate dramatically

from the initial configuration. This is reflected in the C $\alpha$  RMSD and the gyration radius shown in Figure 2(a and b, respectively). These changes resulted in a fully open structure similar to that obtained previously by Scott and Schiffer<sup>54</sup> (without counterions). Comparing this fully open conformation with the starting structure, it can be seen that the secondary and tertiary structural elements are affected only slightly (Fig. 2 of Supplemental Material). Most differences occur at the dimerization interface.

### CONCLUSIONS

We have presented a systematic analysis of the effect of changing pH on the structural stability of the free HIV-1 protease using MD techniques. Specifically, we have investigated the structural and dynamic differences between the protease with the monoprotinated and deprotonated catalytic dyad under physiological salt concentrations. It was found that when residues Asp25 and Asp25' are both deprotonated, as they would be at neutral pH, the dynamics and structural stability are extremely sensitive to the presence of counterions. The MD simulations and ab initio calculations suggest that when a  $\text{Na}^+$  ion binds to the catalytic dyad, the configuration of the active site is almost identical to that of the monoprotinated catalytic dyad. The simulations suggest that  $\text{Na}^+$  may act to stabilize the protease at neutral pH, and that the protein will be less stable at low ionic strength. In addition, the large structural changes observed in some previous simulations could be attributed to the low salt concentration in the simulations. The results may also have implications for drug design studies. The “self-blocked” conformation that was shown to be stable in the simulations, and could be an alternate target for drug design, suggests that metal-based inhibitors or compounds that carry a positive charge may be effective in stabilizing a closed, inactive form of the enzyme. We note in this regard that a number of  $\text{Cu}^{2+}$ -based inhibitors of HIV protease have recently been proposed (see Lebon et al.<sup>88</sup> and references therein).

### ACKNOWLEDGMENTS

We gratefully acknowledge a generous grant of computer time provided by the company Entry (Kiev, Ukraine; www.entry.kiev.ua). We also gratefully acknowledge O. Ivanova and D. Kanibolotsky for helpful discussion of calculation of the generalized order parameter. H Saint-Martin, M. Platonov, and O. Kornushina are acknowledged for helpful discussions, and we thank SIMU for financial support.

### REFERENCES

1. Wlodawer A, Erickson JW. Structure-based inhibitors of HIV-1 protease. *Annu Rev Biochem* 1993;62:543–585.
2. Ringe D. X-ray structures of retroviral proteases and their inhibitor-bound complexes. *Methods Enzymol* 1994;241:157–177.
3. Wlodawer A, Miller M, Jaskolski M, Sathyanarayana BK, Baldwin E, Weber IT, Selk LM, Clawson L, Schneider J, Kent SB. Conserved folding in retroviral proteases: crystal structure of a synthetic HIV-1 protease. *Science* 1989;245:616–621.
4. Todd MJ, Semo N, Freire E. The structural stability of the HIV-1 protease. *J Mol Biol* 1998;283:475–488.
5. Lange-Savage G, Berchtold H, Liesum A, Budt KH, Peyman A, Knolle J, Sedlacek J, Fabry M, Hilgenfeld R. Structure of HOE/

- BAY 793 complexed to human immunodeficiency virus (HIV-1) protease in two different crystal forms—structure/function relationship and influence of crystal packing. *Eur J Biochem* 1997;248:313–322.
6. Kohl NE, Emini EA, Schleif WA, Davis LJ, Heimbach JC, Dixon RA, Scolnick EM, Sigal IS. Active human immunodeficiency virus protease is required for viral infectivity. *Proc Natl Acad Sci USA* 1988;85:4686–4690.
  7. Hsu I-N, Delbaere LTJ, James MNG, Hofmann T. Penicillopepsin: 2.8 Å structure, active site conformation and mechanistic implications. In: Tang J, editor. *Acid proteases, structure, function, and biology*. New York: Plenum Press; 1977. p 61–81.
  8. Park H, Suh J, Lee S. Ab initio studies on the catalytic mechanism of aspartic proteinases: nucleophilic versus general acid/general base mechanism. *J Am Chem Soc* 2000; 122:3901–3908.
  9. Trylska J, Grochowski P, McCammon JA. The role of hydrogen bonding in the enzymatic reaction catalyzed by HIV-1 protease. *Protein Sci* 2004;13:513–528.
  10. Fruton JS. Aspartyl proteinases. In: Neuberger A, Brocklehurst K, editors. *Hydrolytic enzymes*. Amsterdam: Elsevier; 1987. p 1–37.
  11. Hyland LJ, Tomaszek TA Jr, Meek TD. Human immunodeficiency virus-1 protease: 2. Use of pH rate studies and solvent kinetic isotope effects to elucidate details of chemical mechanism. *Biochemistry* 1991;30:8454–8463.
  12. James MNG, Sielecki AR, Hayakawa K, Gelb MH. Crystallographic analysis of transition state mimics bound to penicillopepsin: difluorostatine- and difluorostatone-containing peptides. *Biochemistry* 1992;31:3872–3886.
  13. Rodriguez EJ, Angeles TS, Meek TD. Use of nitrogen-15 kinetic isotope effects to elucidate details of the chemical mechanism of human immunodeficiency virus 1 protease. *Biochemistry* 1993;32:12380–12385.
  14. Suguna K, Padlan EA, Smith CW, Carlson WD, Davies DR. Binding of a reduced peptide inhibitor to the aspartic proteinase from *Rhizopus chinensis*: implications for a mechanism of action. *Proc Natl Acad Sci USA* 1987;84:7009–7013.
  15. Chatfield DC, Brooks BR. HIV-1 protease cleavage mechanism elucidated with molecular dynamics simulation. *J Am Chem Soc* 1995;117:5561–5572.
  16. Chatfield DC, Eurenium KP, Brooks BR. HIV-1 protease cleavage mechanism: a theoretical investigation based on classical MD simulation and reaction path calculations using a hybrid QM/MM potential. *J Mol Struct (THEOCHEM)* 1998;423:79–92.
  17. Lee H, Darden TA, Pedersen LG. An ab initio quantum mechanical model for the catalytic mechanism of HIV-1 protease. *J Am Chem Soc* 1996;118:3946–3950.
  18. Liu H, Muller-Plathe F, van Gunsteren WF. A combined quantum/classical molecular dynamics study of the catalytic mechanism of HIV protease. *J Mol Biol* 1996;261:454–469.
  19. Silva AM, Cachau RE, Sham HL, Jerickson JW. Inhibition and catalytic mechanism of HIV-1 aspartic protease. *J Mol Biol* 1996;255:321–346.
  20. Venturini A, Lopez-Ortiz F, Alvarez JM, Gonzalez J. Theoretical proposal of a catalytic mechanism for the HIV-1 protease involving an enzyme-bound tetrahedral intermediate. *J Am Chem Soc* 1998;120:1110–1111.
  21. Okimoto N, Tsukui T, Hata M, Hoshino T, Tsuda M. Hydrolysis mechanism of the phenylalanine-proline peptide bond specific to HIV-1 protease: investigation by the ab initio molecular orbital method. *J Am Chem Soc* 1999;121:7349–7354.
  22. Trylska J, Bala P, Geller M, Grochowski P. Molecular dynamics simulations of the first steps of the reaction catalyzed by HIV-1 protease. *Biophys J* 2002;83:794–807.
  23. Billich A, Hammerschmid F, Winkler G. Purification, assay and kinetic features of HIV-1 proteinase. *Biol Chem Hoppe Seyler* 1990;371:265–272.
  24. Ido E, Han HP, Kezdy FJ, Tang J. Kinetic studies of human immunodeficiency virus type 1 protease and its active-site hydrogen bond mutant A28S. *J Biol Chem* 1991;266:24359–24366.
  25. Polgar L, Szeltner Z, Boros I. Substrate-dependent mechanisms in the catalysis of human immunodeficiency virus protease. *Biochemistry* 1994;33:9351–9357.
  26. Piana S, Sebastiani D, Carloni P, Parrinello M. Ab initio molecular dynamics based assignment of the protonation state of pepstatin A/HIV-1 protease cleavage site. *J Am Chem Soc* 2001;123:8730–8737.
  27. Smith R, Breton IM, Chai RY, Kent SBH. Ionization states of the catalytic residues in HIV-1 protease. *Nat Struct Biol* 1996;3:946–950.
  28. Yamazaki T, Nicholson LK, Torchia DA, Wingfield P, Stahl SJ, Kaufman JD, Eyermann CJ, Hodge CN, Lam PYS, Ru Y, Jadhav PK, Chang C, Weber PC. NMR and X-ray evidence that the HIV protease catalytic aspartyl groups are protonated in the complex formed by the protease and a non-peptide cyclic urea-based inhibitor. *J Am Chem Soc* 1994;116:10791–10792.
  29. Wang YX, Freedberg DI, Yamazaki T, Wingfield PT, Stahl SJ, Kaufman JD, Kiso Y, Torchia DA. Solution NMR evidence that the HIV-1 protease catalytic aspartyl groups have different ionization states in the complex formed with the asymmetric drug KNI-272. *Biochemistry* 1996;35:9945–9950.
  30. Harte WE Jr, Beveridge DL. Prediction of the protonation state of the active site aspartyl residues in HIV-1 protease-inhibitor complexes via molecular dynamics simulation. *J Am Chem Soc* 1993;115:3883–3886.
  31. Trylska J, Antosiewicz J, Geller M, Hodge CN, Klabe RM, Head MS, Gilson MK. Thermodynamic linkage between the binding of protons and inhibitors to HIV-1 protease. *Protein Sci* 1999;8:180–195.
  32. Piana S, Carloni P. Conformational flexibility of the catalytic Asp dyad in HIV-1 protease: an ab initio study on the free enzyme. *Proteins* 2000;39:26–36.
  33. Geller M, Miller M, Swanson SM, Maizel J. Analysis of the structure of HIV-1 protease complexed with a hexapeptide inhibitor: Part II. Molecular dynamics studies of the active site region. *Proteins* 1997;27:195–203.
  34. Northrop DB. Follow the protons: a low-barrier hydrogen bond unifies the mechanisms of the aspartic proteases. *Acc Chem Res* 2001;34:790–797.
  35. Tawa GJ, Topol IA, Burt SK, Erickson JW. Calculation of relative binding free energies of peptidic inhibitors to HIV-1 protease and its I84V mutant. *J Am Chem Soc* 1998;120:8856–8863.
  36. Xie D, Gulnick S, Collins L, Gustchina E, Suvorov L, Erickson JW. Dissection of the pH dependence of inhibitor binding energetics for an aspartic protease: direct measurements of the protonation states of the catalytic aspartic acid residues. *Biochemistry* 1997;36:16166–16172.
  37. Gomez J, Freire E. Thermodynamic mapping of the inhibitor site of the aspartic protease endothiapepsin. *J Mol Biol* 1995;252:337–350.
  38. Mardis KL, Luo R, Gilson MK. Interpreting trends in the binding of cyclic ureas to HIV-1 protease. *J Mol Biol* 2001;309:507–517.
  39. Todd MJ, Freire E. The effect of inhibitor binding on the structural stability and cooperativity of the HIV-1 protease. *Proteins* 1999;36:147–156.
  40. Kuzmic P, Garcia-Echeverria C, Rich DH. Stabilization of HIV protease dimer by bound substrate. *Biochem Biophys Res Commun* 1993;94:301–305.
  41. Tyagi SC, Simon SR, Carter CA. Effect of pH and nonphysiological salt concentrations on human immunodeficiency virus-1 protease dimerization. *Biochem Cell Biol* 1994;72:175–181.
  42. Cheng YS, Yin FH, Foundling S, Blomstrom D, Kettner CA. Stability and activity of human immunodeficiency virus protease: comparison of the natural dimer with a homologous, single-chain tethered dimer. *Proc Natl Acad Sci USA* 1990;87:9660–9664.
  43. Rodriguez EJ, Debouck C, Deckman IC, Abu-Soud H, Raushel FM, Meek TD. Inhibitor binding to the Phe53Trp mutant of HIV-1 protease promotes conformational changes detectable by spectrofluorometry. *Biochemistry* 1993;32:3557–3563.
  44. Ullrich B, Laberge M, Tolgyesi F, Szeltner Z, Polgar L, Fidy J. Trp42 rotamers report reduced flexibility when the inhibitor acetyl-pepstatin is bound to HIV-1 protease. *Protein Sci* 2000;9:2232–2245.
  45. Zoete V, Michielin O, Karplus M. Relation between sequence and structure of HIV-1 protease inhibitor complexes: a model system for the analysis of protein flexibility. *J Mol Biol* 2002;315:21–52.
  46. Kurt N, Scott WR, Schiffer CA, Haliloglu T. Cooperative fluctuations of unliganded and substrate-bound HIV-1 protease: a structure-based analysis on a variety of conformations from crystallography and molecular dynamics simulations. *Proteins* 2003;51:409–422.
  47. Zhu Z, Schuster DI, Tuckerman ME. Molecular dynamics study of the connection between flap closing and binding of fullerene-based



- inhibitors of the HIV-1 protease. *Biochemistry* 2003;42:1326–1333.
48. Katoh E, Louis JM, Yamazaki T, Gronenborn AM, Torchia DA, Ishima R. A solution NMR study of the binding kinetics and the internal dynamics of an HIV-1 protease-substrate complex. *Protein Sci* 2003;12:1376–1385.
  49. Rick SW, Erickson JW, Burt SK. Reaction path and free energy calculations of the transition between alternate conformations of HIV-1 protease. *Proteins* 1998;32:7–16.
  50. Venable RM, Brooks BR, Carson FW. Theoretical studies of relaxation of a monomeric subunit of HIV-1 protease in water using molecular dynamics. *Proteins* 1993;15:374–384.
  51. Harte WE Jr, Swaminathan S, Mansuri MM, Martin JC, Rosenberg IE, Beveridge DL. Domain communication in the dynamical structure of human immunodeficiency virus 1 protease. *Proc Natl Acad Sci USA* 1990;87:8864–8868.
  52. Wang W, Kollman PA. Free energy calculations on dimer stability of the HIV protease using molecular dynamics and a continuum solvent model. *J Mol Biol* 2000;303:567–582.
  53. Collins JR, Burt SK, Erickson JW. Flap opening in HIV-1 protease simulated by “activated” molecular dynamics. *Nat Struct Biol* 1995;2:334–338.
  54. Scott WR, Schiffer CA. Curling of flap tips in HIV-1 protease as a mechanism for substrate entry and tolerance of drug resistance. *Struct Fold Des* 2000;8:1259–1265.
  55. Ishima R, Freedberg DI, Wang YX, Louis JM, Torchia DA. Flap opening and dimer-interface flexibility in the free and inhibitor-bound HIV protease, and their implications for function. *Struct Fold Des* 1999;7:1047–1055.
  56. Freedberg DI, Ishima R, Jacob J, Wang YX, Kustanovich I, Louis JM, Torchia DA. Rapid structural fluctuations of the free HIV protease flaps in solution: relationship to crystal structures and comparison with predictions of dynamics calculations. *Protein Sci* 2002;11:221–232.
  57. Kurt N, Scott WR, Schiffer CA, Haliloglu T. Cooperative fluctuations of unliganded and substrate-bound HIV-1 protease: a structure-based analysis on a variety of conformations from crystallography and molecular dynamics simulations. *Proteins* 2003;51:409–422.
  58. Berendsen HJC, van der Spoel D, van Drunen R. GROMACS: a message-passing parallel molecular dynamics implementation. *Comp Phys Comm* 1995;91:43–56.
  59. Lindahl E, Hess B, van der Spoel D. GROMACS 3.0: a package for molecular simulation and trajectory analysis. *J Mol Mod* 2001;7:306–317.
  60. Schuler LD, Daura X, van Gunsteren WF. An improved GROMOS96 force field for aliphatic hydrocarbons in the condensed phase. *J Comput Chem* 2001;22:1205–1218.
  61. Verlet L. Computer experiments on classical fluids: I. Thermodynamical properties of Lennard–Jones molecules. *Phys Rev* 1967;159:98–103.
  62. Essman U, Perela L, Berkowitz ML, Darden T, Lee H, Pedersen LG. A smooth particle mesh Ewald method. *J Chem Phys* 1995;103:8577–8592.
  63. Ryckaert JR, Ciccotti G, Berendsen HJC. Numerical integration of the Cartesian equations of motion of a system with constraints: molecular dynamics of n-alkanes. *J Comp Phys* 1977;23:327–341.
  64. Miyamoto S, Kollman PA. SETTLE: an analytical version of the SHAKE and RATTLE algorithms for rigid water models. *J Comp Chem* 1992;13:952–962.
  65. Berendsen HJC, Postma JPM, DiNola A, Haak JR. Molecular dynamics with coupling to an external bath. *J Chem Phys* 1984;81:3684–3690.
  66. Spinelli S, Liu QZ, Alzari PM, Hirel PH, Poljak RJ. The three-dimensional structure of the aspartyl protease from the HIV-1 isolate BRU. *Biochimie* 1991;73:1391–1396.
  67. Bernstein FC, Koetzle TF, Williams GJ, Meyer EF Jr, Brice MD, Rodgers JR, Kennard O, Shimanouchi T, Tasumi M. The Protein Data Bank: a computer-based archival file for macromolecular structures. *Eur J Biochem* 1977;80:319–324.
  68. Berendsen HJC, Postma JPM, van Gunsteren WF, Hermans J. Interaction models for water in relation to protein hydration. In: Pullman B, editor. *Intermolecular forces*. Dordrecht: Reidel; 1981. p 331–342.
  69. Granovsky AA. PC GAMESS. Available online at <http://classic.chem.msu.su/gran/games/index.html>
  70. Schmidt MW, Baldrige KK, Boatz JA, Elbert ST, Gordon MS, Jensen JJ, Koseki S, Matsunaga N, Nguyen KA, Su S, Windus TL, Dupuis M, Montgomery JA. General atomic and molecular electronic structure system. *J Comput Chem* 1993;14:1347–1363.
  71. Hehre WJ, Ditchfield R, Pople JA. Self-consistent molecular orbital methods: XII. Further extensions of Gaussian-type basis sets for use in molecular orbital studies of organic molecules. *J Chem Phys* 1972;56:2257–2261.
  72. Francl MM, Pietro WJ, Hehre WJ, Binkley JS, Gordon MS, DeFrees DJ, Pople JA. Self-consistent molecular orbital methods: XXIII. Polarization-type basis set of second row elements. *J Chem Phys* 1982;77:3654–3665.
  73. Frisch MJ, Pople JA, Binkley JS. Self-consistent molecular orbital methods: XXV. Supplementary functions for Gaussian basis sets. *J Chem Phys* 1984;80:3265–3269.
  74. Lipari G, Szabo A. Model free approach to the interpretation of nuclear magnetic resonance relaxation in macromolecules: 2. Analysis of experimental results. *J Am Chem Soc* 1982;104:4559–4570.
  75. Lipari G, Szabo A. Model free approach to the interpretation of nuclear magnetic resonance relaxation in macromolecules: 1. Theory and range of validity. *J Am Chem Soc* 1982;104:4546–4559.
  76. Eriksson MA, Berglund H, Hard T, Nilsson L. A comparison of <sup>15</sup>N NMR relaxation measurements with a molecular dynamics simulation: backbone dynamics of the glucocorticoid receptor DNA-binding domain. *Proteins* 1993;17:375–390.
  77. Guex N, Peitsch MC. SWISS-MODEL and the Swiss-PdbViewer: An environment for comparative protein modeling. *Electrophoresis* 1997;18:2714–2723.
  78. Portmann S, Lüthi HP. MOLEKEL: An interactive molecular graphics tool. *CHIMIA* 2000;54:766–770.
  79. Humphrey W, Dalke A, Schulten K. VMD—visual molecular dynamics. *J Mol Graphics* 1996;14:33–38.
  80. Nayal M, Di Cera E. Valence screening of water in protein crystals reveals potential Na<sup>+</sup> binding sites. *J Mol Biol* 1996;256:228–234.
  81. Kabsch W, Sander C. Dictionary of protein secondary structure: pattern recognition of hydrogen-bonded and geometrical features. *Biopolymers* 1983;22:2577–2637.
  82. Xie D, Gulnik S, Gustchina E, Yu B, Shao W, Qoronfeh W, Nathan A, Erickson JW. Drug resistance mutations can effect dimer stability of HIV-1 protease at neutral pH. *Protein Sci* 1999;8:1702–1707.
  83. Harrison RW, Weber IT. Molecular dynamics simulations of HIV-1 protease with peptide substrate. *Protein Eng* 1994;7:1353–1363.
  84. Vondrasek J, van Buskirk CP, Wlodawer A. Database of three-dimensional structures of HIV proteinases. *Nat Struct Biol* 1997;4:8.
  85. Woon TC, Brinkworth RI, Fairlie DP. Inhibition of HIV-1 proteinase by metal ions. *Int J Biochem* 1992;24:911–914.
  86. Zhang ZY, Reardon IM, Hui JO, O’Connell KL, Poorman RA, Tomasselli AG, Heinrichson RL. Zinc inhibition of renin and the protease from human immunodeficiency virus type 1. *Biochemistry* 1991;30:8717–21.
  87. York DM, Darden TA, Pedersen LG, Anderson MW. Molecular modeling studies suggest that zinc ions inhibit HIV-1 protease by binding at catalytic aspartates. *Environ Health Perspect* 1993;101:246–250.
  88. Lebon F, Boggetto N, Ledecq M, Durant F, Benatallah Z, Sicsic S, Lapouyade R, Kahn O, Mouithys-Mickalad A, Deby-Dupont G, Reboud-Ravaux M. Metal-organic compounds: a new approach for drug discovery. N1-(4-methyl-2-pyridyl)-2,3,6-trimethoxybenzamide copper(II) complex as an inhibitor of human immunodeficiency virus 1 protease. *Biochem Pharmacol* 2002;63:1863–1873.